



THE UNIVERSITY *of* EDINBURGH

Edinburgh Research Explorer

An Interfacial Layer based on Polymer of Intrinsic Microporosity to Suppress Dendrite Growth on LiMetal Anodes

Citation for published version:

Qi, L, Shang, L, Wu, K, Qu, L, Pei, H, Li, W, Zhang, L, Wu, Z, Zhou, H, Mckeown, NB, Zhang, W & Yang, Z 2019, 'An Interfacial Layer based on Polymer of Intrinsic Microporosity to Suppress Dendrite Growth on Li Metal Anodes', *Chemistry - A European Journal*. <https://doi.org/10.1002/chem.201902124>

Digital Object Identifier (DOI):

[10.1002/chem.201902124](https://doi.org/10.1002/chem.201902124)

Link:

[Link to publication record in Edinburgh Research Explorer](#)

Document Version:

Peer reviewed version

Published In:

Chemistry - A European Journal

General rights

Copyright for the publications made accessible via the Edinburgh Research Explorer is retained by the author(s) and / or other copyright owners and it is a condition of accessing these publications that users recognise and abide by the legal requirements associated with these rights.

Take down policy

The University of Edinburgh has made every reasonable effort to ensure that Edinburgh Research Explorer content complies with UK legislation. If you believe that the public display of this file breaches copyright please contact openaccess@ed.ac.uk providing details, and we will remove access to the work immediately and investigate your claim.



COMMUNICATION

An Interfacial Layer based on Polymer of Intrinsic Microporosity to Suppress Dendrite Growth on Li-Metal Anodes

Liya Qi^{# [a,b,c]}, Luoran Shang^{# [a,d]}, Kai Wu^[b], Liangliang Qu^[a], Hao Pei^[a], Wen Li^[a,e], Lexiang Zhang^[a], Zhengwei Wu^[a,f], Henghui Zhou^{*[b]}, Neil B McKeown^{*[g]}, Weixia Zhang^{*[a]}, Zhengjin Yang^{*[h]}

Abstract: The performance and safety of lithium (Li) metal batteries can be compromised due to the formation of Li dendrites. Here we report the use of a polymer of intrinsic microporosity (PIM) as a feasible and robust interfacial layer that inhibits dendrite growth. The PIM demonstrates excellent film-forming ability, electrochemical stability, strong adhesion to a copper metal electrode and outstanding mechanical flexibility so that it relieves the stress of structural changes produced by reversible lithiation. Importantly, the porous structure of the PIM, which guides Li flux to obtain uniform deposition, and its strong mechanical strength combine to suppress dendrite growth. Hence, the electrochemical performance of the anode is significantly enhanced, promising excellent performance and extended cycle lifetime of Li-metal batteries.

Lithium (Li) batteries are proposed to meet the ever-increasing demand for effective energy storage required for portable electronics and electric vehicles due to their high energy density.^[1] Considerable efforts have been devoted to improving the

performance of Li batteries. Particularly, the anode that plays an important role in determine the overall performance of a battery has attracted more research interests. Li metal is considered to be an exceptional anode material for the next-generation of high energy density batteries, such as Li-S and Li-air batteries,^[2] mainly because of its high theoretical capacity (3860 mA h g⁻¹) and low electrochemical potential (-3.04 V vs the standard hydrogen electrode)^[3]. In spite of much progress in their development, Li anodes still suffer from severe safety problems related to Li dendrite growth upon repeated charging and discharging, which arises from the non-uniform Li deposition across the electrode surface, as represented in Scheme 1a. Such dendrites impair performance and can short circuit the battery causing catastrophic failure,^[4] thus greatly hinder large-scale commercial application of Li metal anodes in batteries.

To solve the problem of dendrite formation, several approaches have been developed, such as engineering electrolytes, guiding Li ion flux, and coating an interfacial layer. For instance, engineering electrolytes by employing solid electrolytes or by using additives to improve the uniformity at the in-situ formed solid electrolyte interface (SEI) can suppress Li dendrite growth^[5]. However, it usually requires long and tedious screening work to find the best electrolyte/additive/anode combination, and also may lead to low power output because of low ionic conductivity and large interfacial resistance caused by solid electrolytes^[6], or has limited success due to consumption of the additives when cycling over long periods of time^[7]. Moreover, the underlying mechanism of how the electrolyte and the electrode compositions influence the formation and the morphology of the SEI layer is not clear, preventing the reproducible massive-scale application.^[8] Guiding Li ion flux by creating patterned nanostructures to ensure uniform Li deposition is beneficial; for instance, the incorporation of 2D boron nitride nanoflakes substantially improves the Li⁺ transference number and suppressed Li-dendrite formation.^[9] However, the fabrication process was complicated and hence expensive.^[10]

The introduction of an interfacial layer to stabilize the interface between Li metal and electrolytes can suppress Li dendrite growth. Coating an interfacial layer is typically a scalable process with compatibility with different electrolytes, providing a complementary approach to the development of new electrolytes for Li metal anodes^[11]. An ideal interfacial layer for the Li metal anode is electrochemically stable in the highly reducing environment and also mechanically strong to block the formation of Li dendrites.^[6c] Previously investigated interfacial layers composed of, for example, a diamond-like carbon film, interconnected hollow carbon nanospheres, Al₂O₃, polymers,^[12] and HF modified poly(dimethylsiloxane) film,^[6c, 11a, 11c, 13] all tend to rely on complex processing, involving sophisticated apparatus or toxic chemicals. Therefore, new interfacial layer materials that

- [a] Dr. L. Qi, Dr. L. Shang, Dr. L. Qu, Dr. H. Pei, Dr. W. Li, Dr. L. Zhang, Z. Wu, Dr. W. Zhang*
John A. Paulson School of Engineering and Applied Sciences, Harvard University, Cambridge, MA, 02138, United States
E-mail: wxzhang@seas.harvard.edu
- [b] Dr. L. Qi, K. Wu, Dr. H. Zhou*
College of Chemistry and Molecular Engineering, Peking University, Beijing, 100871, China
E-mail: hhzhou@pku.edu.cn
- [c] Dr. L. Qi
Beijing Institute of Chemical Industry, Sinopec, Beijing, 100010, China,
- [d] Dr. L. Shang
Institutes of Biomedical Sciences, Fudan University, Shanghai, 200032, China
- [e] Dr. W. Li
School of Materials Science & Engineering, Department of Polymer Materials, Shanghai University, Shanghai, 200444, China,
- [f] Z. Wu
Department of Biomedical Engineering and Biotechnology, University of Massachusetts Lowell, Lowell, MA, 01854, United States
- [g] Dr. N. B. McKeown*
EaStCHEM School of Chemistry, University of Edinburgh, David Brewster Road, Edinburgh, EH9 3FJ, U.K
E-mail: neil.mckeown@ed.ac.uk
- [h] Dr. Z. Yang*
CAS Key Laboratory of Soft Matter Chemistry, Collaborative Innovation Centre of Chemistry for Energy Materials, School of Chemistry and Material Science, University of Science and Technology of China, Hefei, 230026, China
E-mail: yangzj09@ustc.edu.cn

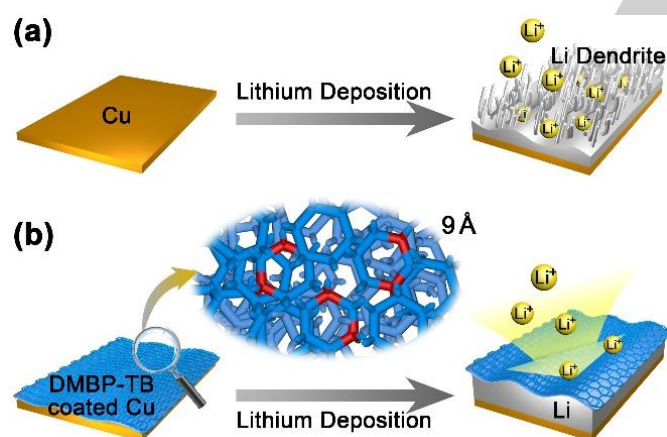
These authors contribute equally.

Supporting information for this article is given via a link at the end of the document.

COMMUNICATION

can be readily processed to fabricate an effective interfacial layer are urgently required to aid the development of Li metal batteries.

Here we report a thin, robust and flexible interfacial layer with 3D interconnected pores based on a polymer of intrinsic microporosity (PIM) that efficiently inhibits Li dendrite formation and growth (Scheme 1b). The PIM used here, PIM-DMBP-TB, features intrinsic microporosity, can be well dissolved in common organic solvents and exhibits excellent film-forming property, thereby enabling a massive-scale application via a simple spin-coating method. We demonstrated that the DMBP-TB artificial layer is stable and has excellent mechanical flexibility and a high Young's modulus that is enough to suppress Li dendrite growth^[6b, 6c]. In addition, the DMBP-TB film has uniform well-interconnected pores, providing uniform conduction of Li ions. Our results confirm that the Li deposition takes place underneath the PIM interfacial layer without Li dendrites growth, stabilizing the electrochemical performance and significantly extending the cycle lifetime of Li metal anode. In contrast to the fast capacity fade due to Li-dendrite formation of the bare Li-anode, the PIM-DMBP-TB coated Li-anode provides stable performance over 200 continuous cycles, maintaining a coulombic efficiency of ~98.3%, without noticeable capacity fade. A full cell assembled with LiFePO₄ cathode and the PIM-DMBP-TB coated Li metal anode delivers stable performance over 100 cycles and has a coulombic efficiency of ~100%.



Scheme 1. Schematic illustration of Li deposition on different substrates. (a) On a bare Cu electrode with Li dendrites after many cycles. (b) Guided deposition through a PIM-DMBP-TB coated Cu electrode with suppressed Li dendrite formation.

PIM-DMBP-TB (Figure 1a) consists of dimethylbiphenyl (DMBP) structural units fused together by the Tröger's base linkage (TB). It was synthesized readily from a commercially available precursor, 4,4'-diamino-3,3'-dimethylbiphenyl, using the previously reported TB polymerization method.^[14] The resulting polymer was characterized structurally using ¹H-NMR and gel permeation chromatography, which gave a weight average molecular mass of 61 kmol g⁻¹ relative to polystyrene standards (Supporting Information and Scheme S1, Figure S1 and S2).^[14c] The rigid V-shape bridged bicyclic TB linkage in the polymer

backbone (Figure 1a) imparts the polymer with intrinsic microporosity by preventing efficient chain packing.^[15] The BET surface of PIM-DMBP-TB was determined as 340 m² g⁻¹ using nitrogen adsorption at 77 K. Analysis of the low-pressure adsorption data indicated an average pore size of ~ 9 Å (Figure S3), which is much larger than the diameter of Li ions (~ 1.8 Å) and Li atoms (~ 2.7 Å). The ion conductivity of PIM-DMBP-TB was measured to be 4.41×10⁻⁴ S cm⁻¹ at 20 °C based on EIS spectra (Figure S4). Considering the pore size of PIM-DMBP-TB, the polymer film can only allow the transport of the less solvated lithium ion instead of the fully solvated ones^[16]. The PIM-DMBP-TB acts as a sieve which consequently can greatly restrain the unfavourable reaction between the Li metal and the electrolyte. PIM-DMBP-TB is thermally stable up to 400 °C (Figure S5), which is sufficient for Li metal battery applications. In addition, PIM-DMBP-TB is highly soluble in common organic solvents, such as chloroform, from which it is solution processable. A flexible film can be easily fabricated by casting from solution as shown in Figure 1b and Figure S6, S7. The modulus of the free-standing PIM-DMBP-TB film is ~ 9 GPa, a value which is significantly higher than the 6 GPa reported to be the minimum required to suppress Li dendrite growth.^[6b, 6c]

Spin-coating was used to coat a PIM-DMBP-TB interfacial layer with a thickness of 2 μm on a copper (Cu) current collector (Figure S6). Analysis of the scanning electron micrographs of the coated Cu electrode confirms the thickness of the layer and a uniformly flat morphology (Figure 1c and 1d). The robustness of the PIM-DMBP-TB coated Cu electrode was tested by being repeatedly folded. Digital camera photos and optical images of the coated Cu electrode indicate few cracks on the interfacial layer and no obvious delamination of the polymer (Figure S8). This illustrates the excellent mechanical flexibility of the PIM-DMBP-TB layer and strong adhesion between the coating layer and the Cu electrode. These properties are important for relieving stress generated from the volume changes resulting from reversible lithiation during charging/discharging.

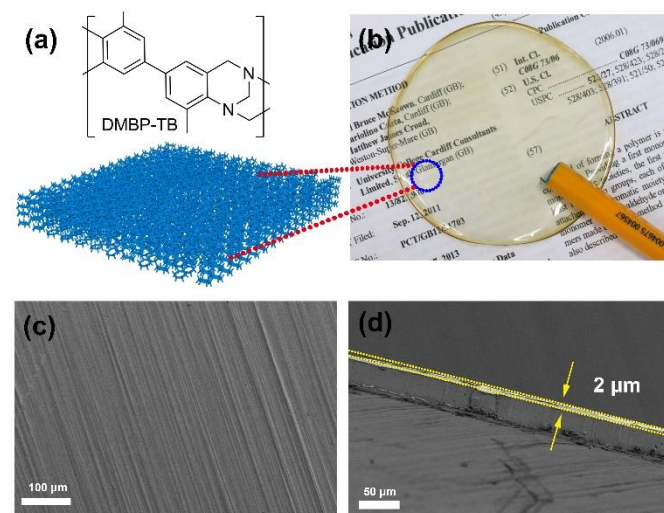


Figure 1. (a) Structure of PIM-DMBP-TB. (b) A free-standing transparent PIM-DMBP-TB film from solution casting. The 3D interconnected porous structure as illustrated can provide evenly distributed Li⁺ conductive pathways. (c) Top view

COMMUNICATION

and (d) cross-sectional SEM image of the PIM-DMBP-TB coating layer ($\sim 2 \mu\text{m}$ thick) on a Cu electrode with neat and flat surface morphology.

To study the electrochemical performance of the PIM-DMBP-TB coated anode, battery cells were assembled with Li metal foil as the counter electrode and an ether-based electrolyte. A control cell was also constructed with an uncoated Cu foil as the working electrode. After 50 continuous stripping/plating cycles at a current density of 0.50 mA cm^{-2} with plating Li metal on anodes to an area-specific capacity of 1.0 mA h cm^{-2} , the morphologies of the Li deposition on the coated and uncoated Cu current collectors were characterized using SEM. For the uncoated Cu current collector, both the cross-sectional and top view SEM images show an uneven surface with wire-like Li filaments clearly observed, indicating the rapid dendritic growth of the deposited Li metal, which breaks the SEI film, as shown in Figure 2a and 2c. This result agrees with previous reports.^[6c, 11a] In contrast, the PIM-DMBP-TB coated current collector has a smooth and flat surface and Li metal is deposited underneath the coating layer without obvious dendrites (Figure 2b and 2d). **The reason is because, by coating the PIM-DMBP-TB polymer on the electrode, we introduce a stable and uniform artificial SEI layer, instead of the native unstable SEI. This thin artificial layer with uniform well-interconnected porous structure and high mechanical modulus can greatly improve the interfacial stability of Li metal anodes, by providing uniform conduction of Li ions and mechanically suppressing the further growth of Li dendrites. Besides, the flexibility of this thin layer can relieve the stress from the volum changes produced by lithiation. Thus, a smooth and flat surface without obvious dendrites can be observed with the PIM-DMBP-TB coating.** The PIM interfacial layer shows very little variation after long cycles of stripping/plating, indicating its good electrochemical stability. Therefore, the prevention of Li dendrites can be attributed both to the high modulus of the PIM-DMBP-TB film that acts as a robust physical shield and its 3D interconnected porosity, which guides Li flux during stripping/plating.

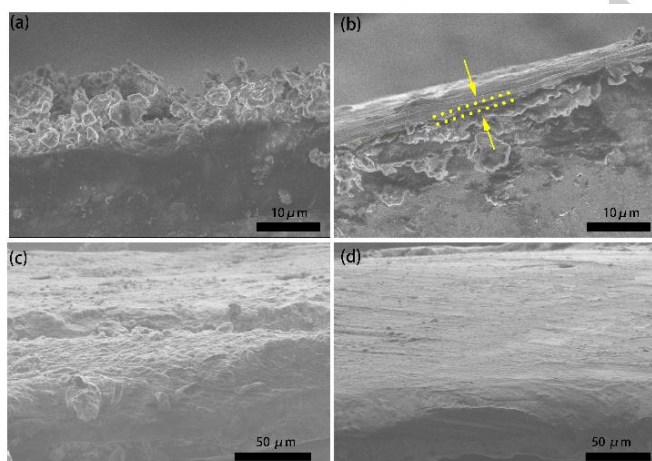


Figure 2. SEM images of uncoated (a,c) and PIM-DMBP-TB coated (b,d) Cu electrodes after 50 cycles of 1 mA h cm^{-2} Li deposition at a current density of 0.5 mA cm^{-2} . Cross-sectional SEM images of deposited Li on

(a) a bare Cu electrode and (b) the PIM-DMBP-TB coated Cu electrode. Top-view SEM images of deposited Li on (c) a bare Cu electrode and (d) the PIM-DMBP-TB coated Cu electrode.

To further explore the inhibitive effect of the PIM-DMBP-TB interfacial layer on the growth of Li dendrites, electrochemical impedance spectroscopic (EIS) measurements were performed, as shown in Figure S9. With continuous cycling, the active surface area increases, leading to reduced interfacial impedances of both anodes. However, the PIM-DMBP-TB coated Cu electrode maintains its semi-circular shape over 80 continuous cycles, implying a relatively stable interface between the electrode and electrolytes. In contrast, for the uncoated Cu electrode after 80 cycles, the original shape of the spectrum is changed and splits into two separate semicircles, which can be attributed to two different electrochemical processes occurring, firstly, at the electrode/electrolyte interface and, secondly, at the interface between the Li dendrites and electrolyte, implying the growth of Li dendrites on the uncoated Cu electrode.

A comparison of the electrochemical performances, including Coulombic efficiency (CE), voltage profile and hysteresis, of the control uncoated and PIM-DMBP-TB coated electrodes was achieved using galvanostatic cycling. CE, defined as the ratio of the amount of stripped Li to the amount of Li plated on the Cu electrode in each cycle, is an important parameter for determining cycle life-time. CE for both cells, as a function of cycle number at various current densities, are shown in Figure 3a. For cells with PIM-DMBP-TB coated anode, the CE is stable at $\sim 98.3\%$ over 200 cycles at 0.5 mA cm^{-2} , 97.5% over 150 cycles at 2 mA cm^{-2} , and 95.4% over 100 cycles at 4 mA cm^{-2} , respectively (Figure 3a). Additional CE curves at 1 mA cm^{-2} and 3 mA cm^{-2} are shown in Figure S10. These values of CE for the cell incorporating the PIM-DMBP-TB coated electrode, fabricated by a simple spin-coating method, is comparable to or even better than those based on electrodes with coatings fabricated from more complicated procedures.^[6c, 11a, 17] In comparison, the control cell with the uncoated electrode exhibits a quick decay in CE and short cycle life. At a low current density of 0.5 mA cm^{-2} , the average CE is $\sim 98\%$ for the first 100 cycles but drops below 70% after another 50 cycles. With a higher current density of 2 mA cm^{-2} , the CE decreases rapidly to 90% after 120 cycles and degrades suddenly afterwards with a large fluctuation. After 150 cycles, the CE is less than 50% because of severe formation of “dead” Li. As the current density is further increased to 3 or 4 mA cm^{-2} (Figure S10b and Figure 3a), a value required for practical batteries, the performance of the uncoated Li anode degrades further. For the first 50 cycles at 4 mA cm^{-2} , CE was retained at $\sim 90\%$ but then sharply decreases to $<60\%$ after another 30 cycles (Figure 3a). This degradation is caused by severe Li metal dendrite formation induced by the rapid plating of Li atoms, depleting electrolytes so fast that excessive “dead” Li is formed. This result is consistent with a previous study reporting that higher current density could lead to the initiation of Li dendrite formation.^[18]

The significantly improved electrode cycling performance of the PIM-DMBP-TB coated electrode is also reflected in the reduction of polarization (hysteresis) in the voltage profiles during Li deposition/stripping. The Li deposition voltage is approximately -26 mV (versus Li/Li+) for the PIM-DMBP-TB coated electrode and

COMMUNICATION

1 -42 mV (versus Li/Li⁺) for uncoated electrode. The Li stripping
 2 voltage is 23 mV (versus Li/Li⁺) for the PIM-DMBP-TB coated
 3 electrode and 38 mV (versus Li/Li⁺) for uncoated electrode, as
 4 shown in Figure 3b. Thus, the over potential of the PIM-DMBP-
 5 TB coated electrode during Li deposition and stripping is reduced,
 6 compared to that of uncoated electrode. This reduced polarization
 7 is an indication of a stable SEI on the coated electrode.^[19]
 8 Moreover, for the PIM-DMBP-TB coated electrode, the hysteresis
 9 remains almost constant after the initial few cycles (Figure 3c),
 10 which is attributed to the stable SEI layer.^[19] In contrast, the
 11 voltage hysteresis of Li deposition/stripping gradually increases
 12 for the uncoated electrode as the cycle number increases, and
 13 reaches ~170 mV after 150 cycles, indicating an unstable SEI.
 14 Overall, the hysteresis of the PIM-DMBP-TB coated electrode,
 15 only ~55 mV after 200 cycles, is ~3 times smaller than that of the
 16 uncoated electrode (Figure 3c). This can be attributed to the lower
 17 charge transfer and internal resistance benefiting from the thinner
 18 SEI layer^[6c] as a result of the uniform Li deposition on the PIM-
 19 DMBP-TB coated electrode surface.^[10b] To demonstrate the
 20 practical application of this PIM coating, a full cell utilizing a
 21 LiFePO₄ cathode and the PIM-DMBP-TB coated Li metal anode
 22 was assembled. This cell shows a high capacity of 143 mA h g⁻¹
 23 and delivers stable performance over 100 cycles at the current
 24 density of 0.5 C, as shown in Figure S11, which confirms the
 25 benefit of using the PIM coating within a practical Li metal battery.

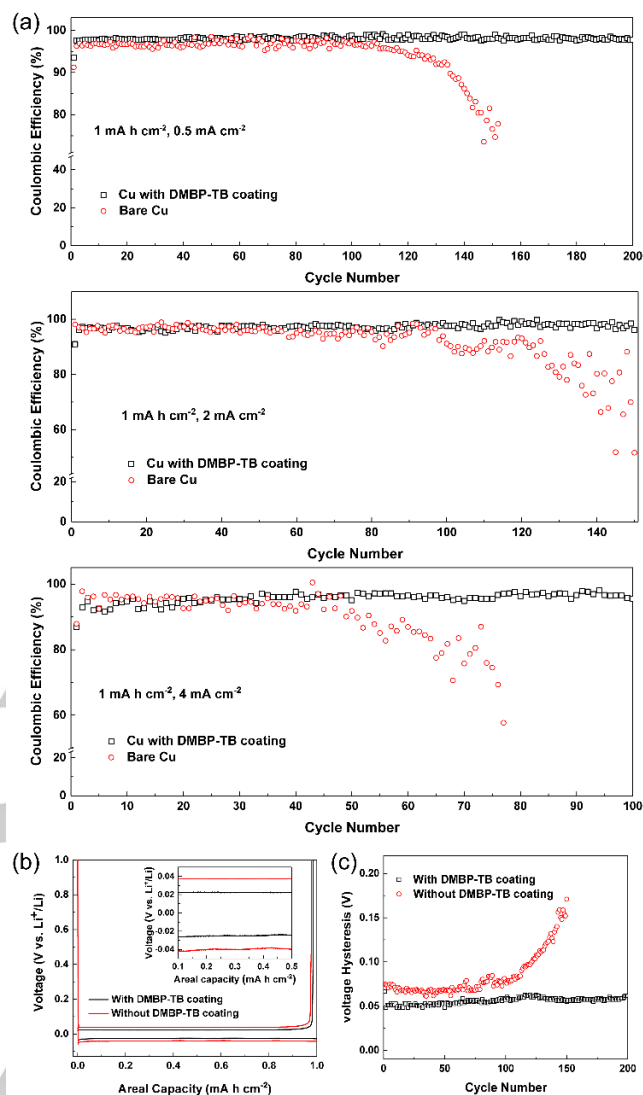


Figure 3. Galvanostatic cycling of Li stripping/plating (discharge/charge) on a bare Cu electrode and the PIM-DMBP-TB coated Cu electrode. (a) Coulombic efficiency for discharging/charging Li on a bare Cu electrode and the PIM-DMBP-TB coated Cu electrode at current densities of 0.5, 2, and 4 mA cm⁻² with total capacity of 1 mA h cm⁻² (b) Discharge/charge voltage profiles for Li stripping/plating on a bare Cu electrode and the PIM-DMBP-TB coated Cu electrode from the 10th cycle, at a current density of 0.5 mA cm⁻². (c) Voltage hysteresis comparison for the Li stripping/plating process on a bare Cu electrode and the PIM-DMBP-TB coated Cu electrode at a current density of 0.5 mA cm⁻².

In summary, we demonstrate that a novel microporous polymer coating on a lithium metal anode provides an interfacial layer that suppresses dendrite growth. This is achieved due to the microporosity of PIM-DMBP-TB, which helps to guide a uniform Li-ion flux during cell cycling, and its high Young's modulus that forms a robust barrier to dendrite growth. The film strongly adheres to the metal electrode surface and is sufficiently flexible to relieve the stress due to the volume changes produced by lithiation. Thus, the PIM-DMBP-TB film appears both mechanically and chemically robust during operation of the cell. In addition, the PIM-DMBP-TB interfacial layer enhances the

1 electrochemical performance of the anode, resulting in improved
 2 CEs and a longer and more stable cycle life. Additionally, the
 3 polymer can be readily coated onto electrodes by simple spin-
 4 coating, a low-cost fabrication process which is compatible with
 5 practical mass production. Therefore, it is anticipated that the use
 6 of PIM-DMBP-TB as an interfacial layer will contribute to the
 7 future development of high-performance Li metal batteries.

11 Acknowledgements

13 Financial support received from the National Science Foundation
 14 of China (No. 21506201) and PULEAD Technology Industry Co.
 15 Ltd is gratefully acknowledged.

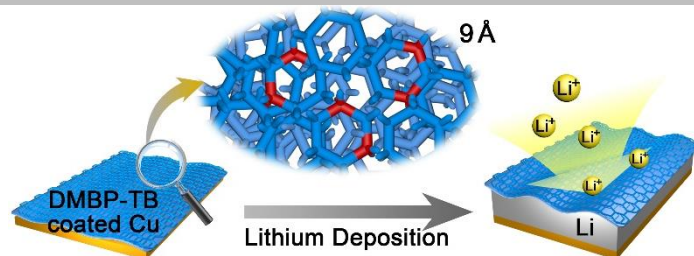
17 **Keywords:** polymer of intrinsic microporosity • Li metal anode •
 18 dendrite • electrochemistry • microporous materials

- [1] J. W. Choi, D. Aurbach, *Nat. Rev. Mater.* **2016**, 1, 16013.
- [2] a) X. Ji, K. T. Lee, L. F. Nazar, *Nat. Mater.* **2009**, 8, 500; b) G. Lorenzo, P. Elie, H. Jusef, P. Jin - Bum, L. Yung - Jung, S. Yang - Kook, P. Stefano, S. Bruno, *Adv. Mater.* **2015**, 27, 784; c) D. Wang, W. Zhang, W. Zheng, X. Cui, T. Rojo, Q. Zhang, *Adv. Sci.* **2017**, 4, 1600168.
- [3] X. Yu, A. Manthiram, *Energy Environ. Sci.* **2018**, 11, 527.
- [4] a) R. Bhattacharyya, B. Key, H. Chen, A. S. Best, A. F. Hollenkamp, C. P. Grey, *Nat. Mater.* **2010**, 9, 504; b) K. J. Harry, D. T. Hallinan, D. Y. Parkinson, A. A. MacDowell, N. P. Balsara, *Nat. Mater.* **2013**, 13, 69.
- [5] a) W. Liu, N. Liu, J. Sun, P.-C. Hsu, Y. Li, H.-W. Lee, Y. Cui, *Nano Lett.* **2015**, 15, 2740; b) N. Kamaya, K. Homma, Y. Yamakawa, M. Hirayama, R. Kanno, M. Yonemura, T. Kamiyama, Y. Kato, S. Hama, K. Kawamoto, A. Mitsui, *Nat. Mater.* **2011**, 10, 682; c) Y. Lu, Z. Tu, L. A. Archer, *Nat. Mater.* **2014**, 13, 961; d) W. Li, H. Yao, K. Yan, G. Zheng, Z. Liang, Y.-M. Chiang, Y. Cui, *Nat. Commun.* **2015**, 6, 7436; e) B. Wu, S. Wang, J. Lochala, D. Desrochers, B. Liu, W. Zhang, J. Yang, J. Xiao, *Energy Environ. Sci.* **2018**, 11, 1803; f) Y. Yang, M. Zhao, H. Geng, Y. Zhang, Y. Fang, C. Li, J. Zhao, *Chemistry – A European Journal* **2019**, 25, 5036; g) C. Zhao, X. Zhang, X. Cheng, R. Zhang, R. Xu, P. Chen, H. Peng, J. Huang, Q. Zhang, *Proc. Natl. Acad. Sci. U.S.A.* **2017**, 114, 11069.
- [6] a) W. Zhou, S. Wang, Y. Li, S. Xin, A. Manthiram, J. B. Goodenough, *J. Am. Chem. Soc.* **2016**, 138, 9385; b) G. M. Stone, S. A. Mullin, A. A. Teran, D. T. Hallinan, A. M. Minor, A. Hexemer, N. P. Balsara, *J. Electrochem. Soc.* **2012**, 159, A222; c) G. Zheng, S. W. Lee, Z. Liang, H. W. Lee, K. Yan, H. Yao, H. Wang, W. Li, S. Chu, Y. Cui, *Nat. Nanotechnol.* **2014**, 9, 618.
- [7] a) F. Ding, W. Xu, G. L. Graff, J. Zhang, M. L. Sushko, X. Chen, Y. Shao, M. H. Engelhard, Z. Nie, J. Xiao, X. Liu, P. V. Sushko, J. Liu, J. G. Zhang, *J. Am. Chem. Soc.* **2013**, 135, 4450; b) W. Liu, D. Lin, A. Pei, Y. Cui, *J. Am. Chem. Soc.* **2016**, 138, 15443.
- [8] S. Jung, Z. L. Brown, J. Kim, B. L. Lucht, *Energy Environ. Sci.* **2018**.
- [9] J. Shim, H. J. Kim, B. G. Kim, Y. S. Kim, D.-G. Kim, J.-C. Lee, *Energy Environ. Sci.* **2017**, 10, 1911.
- [10] a) X. B. Cheng, T. Z. Hou, R. Zhang, H. J. Peng, C. Z. Zhao, J. Q. Huang, Q. Zhang, *Adv. Mater.* **2016**, 28, 2888; b) Z. Liang, G. Zheng, C. Liu, N. Liu, W. Li, K. Yan, H. Yao, P. C. Hsu, S. Chu, Y. Cui, *Nano Lett.* **2015**, 15, 2910; c) S. Chi, Y. Liu, W. Song, L. Fan, Q. Zhang, *Adv. Funct. Mater.* **2017**, 27, 1700348; d) Q. Yun, Y. He, W. Lv, Y. Zhao, B. Li, F. Kang, Q. Yang, *Adv. Mater.* **2016**, 28, 6932; e) L.-L. Lu, J. Ge, J.-N. Yang, S.-M. Chen, H.-B. Yao, F. Zhou, S.-H. Yu, *Nano Lett.* **2016**, 16, 4431; f) L. Liu, Y. Yin, J. Li, N. Li, X. Zeng, H. Ye, Y. Guo, L. Wan, *Joule* **2017**, 1, 563.
- [11] a) B. Zhu, Y. Jin, X. Hu, Q. Zheng, S. Zhang, Q. Wang, J. Zhu, *Adv. Mater.* **2017**, 29; b) Z. Tu, S. Choudhury, M. Zachman, S. Wei, K. Zhang, L. Kourkoutis, L. Archer, *Joule* **2017**, 1, 394; c) N. Li, Y. Shi, Y. Yin, X. Zeng, J. Li, C. Li, L. Wan, R. Wen, Y. Guo, *Angew. Chem. Int. Ed.* **2018**, 57, 1505; d) R. Xu, Y. Xiao, R. Zhang, X. Cheng, C. Zhao, X. Zhang, C. Yan, Q. Zhang, J. Huang, *Adv. Mater.* **2019**, 31, 1808392.
- [12] a) C. B. Bucur, A. Lita, N. Osada, J. Muldoon, *Energy Environ. Sci.* **2016**, 9, 112; b) T. Dong, J. Zhang, G. Xu, J. Chai, H. Du, L. Wang, H. Wen, X. Zang, A. Du, Q. Jia, *Energy Environ. Sci.* **2018**, 11, 1197.
- [13] a) A. A. Arie, J. K. Lee, *Diam. Relat. Mater.* **2011**, 20, 403; b) A. Friesen, S. Hildebrand, F. Horsthemke, M. Börner, R. Klöpsch, P. Niehoff, F. M. Schappacher, M. Winter, *J. Power Sources* **2017**, 363, 70; c) Y. Gao, Y. Zhao, Y. C. Li, Q. Huang, T. E. Mallouk, D. Wang, *J. Am. Chem. Soc.* **2017**, 139, 15288.
- [14] a) M. Carta, R. Malpass-Evans, M. Croad, Y. Rogan, J. C. Jansen, P. Bernardo, F. Bazzarelli, N. B. McKeown, *Science* **2013**, 339, 303; b) M. D. Guiver, Y. M. Lee, *Science* **2013**, 339, 284; c) Z. Yang, R. Guo, R. Malpass-Evans, M. Carta, N. B. McKeown, M. D. Guiver, L. Wu, T. Xu, *Angew. Chem. Int. Ed.* **2016**, 55, 11499.
- [15] a) M. Carta, M. Croad, J. C. Jansen, P. Bernardo, G. Clarizia, N. B. McKeown, *Polym. Chem.* **2014**, 5, 5255; b) M. Carta, M. Croad, R. Malpass-Evans, J. C. Jansen, P. Bernardo, G. Clarizia, K. Friess, M. Lanč, N. B. McKeown, *Adv. Mater.* **2014**, 26, 3526.
- [16] C. Fu, L. Xu, F. W. Aquino, A. v. Cresce, M. Gobet, S. G. Greenbaum, K. Xu, B. M. Wong, J. Guo, *The Journal of Physical Chemistry Letters* **2018**, 9, 1739.
- [17] a) W. Liu, W. Li, D. Zhuo, G. Zheng, Z. Lu, K. Liu, Y. Cui, *ACS Cent. Sci.* **2017**, 3, 135; b) G. Zheng, C. Wang, A. Pei, J. Lopez, F. Shi, Z. Chen, A. D. Sendek, H.-W. Lee, Z. Lu, H. Schneider, M. M. Safont-Sempere, S. Chu, Z. Bao, Y. Cui, *ACS Energy Lett.* **2016**, 1, 1247.
- [18] Y. Guo, H. Li, T. Zhai, *Adv. Mater.* **2017**, 29, 1700007.
- [19] K. Liu, A. Pei, H. R. Lee, B. Kong, N. Liu, D. Lin, Y. Liu, C. Liu, P. C. Hsu, Z. Bao, Y. Cui, *J. Am. Chem. Soc.* **2017**, 139, 4815.

COMMUNICATION

Entry for the Table of Contents

COMMUNICATION



Liya Qi, Luoran Shang, Kai Wu, Liangliang Qu, Hao Pei, Wen Li, Lexiang Zhang, Zhengwei Wu, Henghui Zhou*, Neil B Mckeown*, Weixia Zhang*, Zhengjin Yang*

Page No. – Page No.

An Interfacial Layer based on Polymer of Intrinsic Microporosity to Suppress Dendrite Growth on Li-Metal Anodes

Polymer of intrinsic microporosity for Li dendrite inhibition: A thin, robust and flexible interfacial layer with 3D interconnected pores based on a polymer of intrinsic microporosity (PIM) has been prepared using a simple spin-coating method. The PIM film with unique porous structure and strong mechanical strength of the PIM can sufficiently suppress the dendrite growth on Li-metal anode, resulting a high coulombic efficiency (~ 98.3%) and a long cycle life over 200 cycles

1
2
3
4
5
6
7
8
9
10
11
12
13
14
15
16
17
18
19
20
21
22
23
24
25
26
27
28
29
30
31
32
33
34
35
36
37
38
39
40
41
42
43
44
45
46
47
48
49
50
51
52
53
54
55
56
57
58
59
60
61
62
63
64
65